Application Note
NOV 2023
AN-850-0139

Structural Comparison of the Matrix Metalloproteinase Proenzymes Using Microfluidic Modulation Spectroscopy

- ○ Biosimilars
- ○ mAbs
- ○ ADCs
- ○ AAVs
- ○ Ligand Binding
- ✓ Protein/Peptide Analysis
- ○ VLPs
- ○ Nucleic Acid
- ○ Fusion Proteins
- ✓ Enzyme Analysis

- ⬢ Aggregation
- ⬢ Quantitiation
- ✓ Structure
- ⬢ Stability
- ✓ Similarity

Abstract

Matrix Metalloproteinases (MMPs) are a pressing topic of research. Not only does their study advance our understanding of protein biology, but there is also great interest in developing specific MMP inhibitors for therapeutic applications. To facilitate these research goals, information regarding their structure is vital. In this study, we used Microfluidic Modulation Spectroscopy (MMS) to analyze the structure of MMP-2, MMP-8, and MMP-9 on both our first and second-generation instruments to compare data quality. In addition, we investigated the structural similarities and differences between each of these proteins and found that all three structures were distinct despite the fact that two of the three MMPs are much more similar in their functions compared to the third.

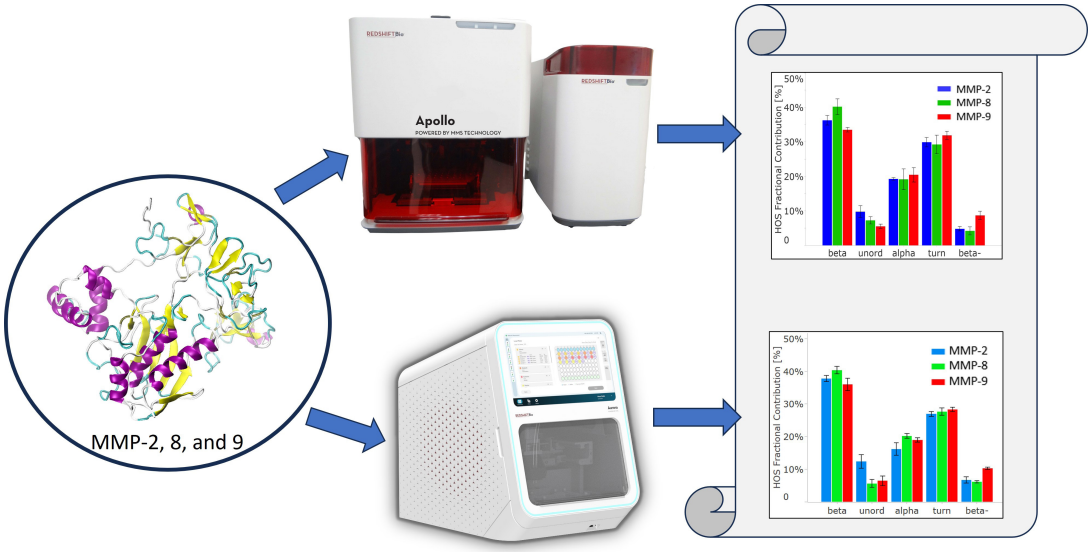

Introduction

Matrix Metalloproteinases (or MMPs) are a class of proteases responsible for the degradation of extracellular matrix (ECM) proteins. Overexpression of certain MMPs is linked to various pathological disorders, including cancer, multiple sclerosis, and strokes.[1] More recently, elevated MMPs have been identified in COVID-19 patients due to their essential roles in lung physiology. [2,3] Consequently, there is significant research interest in utilizing MMPs as biomarkers to predict the severity of COVID-19 and developing inhibitors for targeted treatment strategy in severe cases of the disease.[4] Therefore, understanding the structural variations among different MMPs is essential for advancing this research goal. Various MMPs play distinct roles in ECM tissue remodeling. For example, MMP-8, also known as collagenase 2, digests collagens, while MMP-2 and MMP-9, referred to as gelatinases A and B, respectively, target gelatins. All these MMPs have shown increased expression levels in COVID-19 patients.[2,3] Thus, investigating both the commonalities and differences in the structure of these MMPs will prove invaluable in this context.

REDSHIFTBio®
80 Central Street | Boxborough MA | 01719 | info@redshiftbio.com

Application Note
NOV 2023

Introduction, continued

MMP-2, -8, and -9 have all been extensively studied and structurally characterized particularly in their catalytic forms. The crystal structures of the catalytic domains of these proteins are shown in Figure 1.[6-8] It's evident that the structures of all three proteins are highly similar. The catalytic domains consist of three alpha-helices and five strands of beta-sheets in their secondary structure. The full-length proteins, or proenzymes, of MMP-2 and -9 are shown in Figure 2. Both the pro-domains and the catalytic domains exhibit substantial structural similarities. However, the fibronectin domains differ significantly and are primarily composed of random coils (unordered structures). As of now, the crystal structure of the full-length MMP-8 has not been resolved. In this study, we employed microfluidic modulation spectroscopy (MMS) to characterize and compare the structures of the proenzymes of these MMPs.

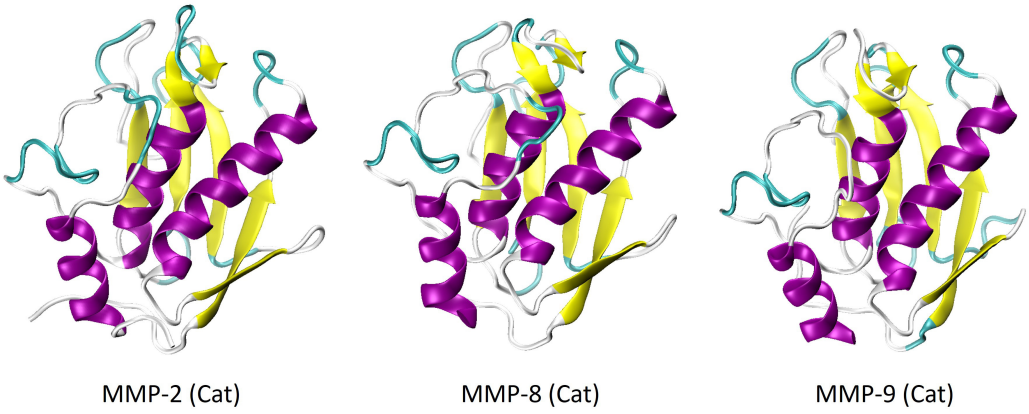

Figure 1. X-ray crystal structures of the catalytic domains of MMP-2 (PDB: 1QIB), MMP-8 (PDB: 2OY4), and MMP-9 (PDB: 1GKC).

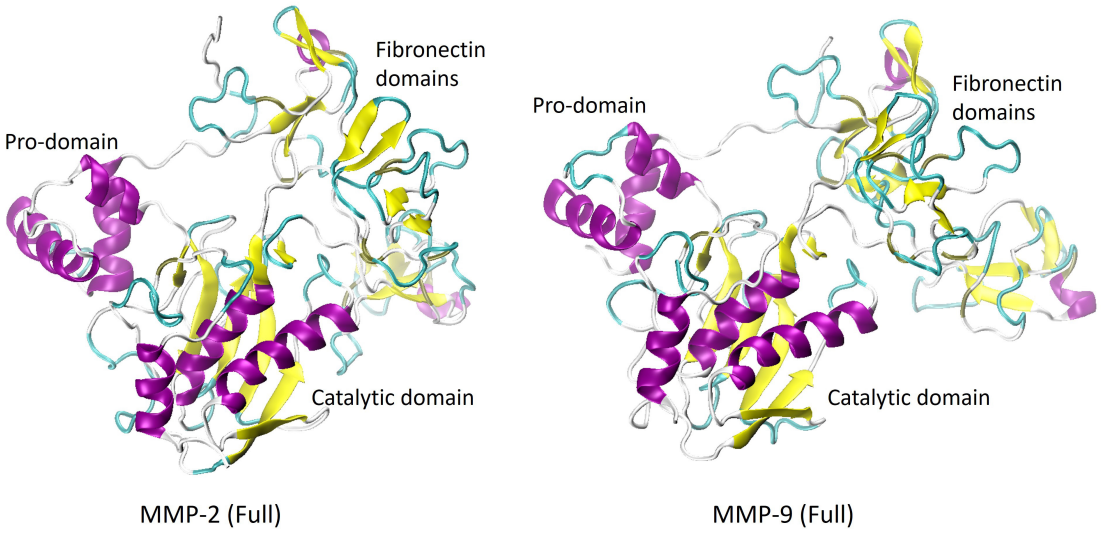

Figure 2. X-ray crystal structures of the full-length proenzymes of MMP-2 (PDB: 1CK7) and MMP-9 (PDB: 1L6J). The C-terminal hemopexin-like domain is not shown.

Application Note
NOV 2023

Introduction, continued

MMS probes the amide I band of the IR spectrum to determine protein structure. To ensure accurate and real-time background subtraction, MMS continuously modulates against the reference buffer. The sensitivity afforded by this technique makes it especially valuable for quality control and is compatible with various formulation buffers. For this study, we employed the first-generation MMS system, Apollo, in addition to our second-generation instrument, Aurora, that significantly minimizes the volume required. Both instruments are equipped with a high-power Quantum Cascade Laser, which, compared to traditional FTIR light sources, is significantly more intense. This increased light intensity, combined with modulating background subtraction makes MMS about 30 times more sensitive than FTIR and 5 times more sensitive than circular dichroism (CD) for detecting small changes in protein structure.[5]

Methods

One milligram each of MMP-2, MMP-8, and MMP-9 were obtained from SinoBiological (Wayne, PA). To ensure buffer matching, MMP-2 and MMP-9 were dialyzed against their respective formulation buffers of 50 mM tris, 150 mM NaCl, 10 mM $CaCl_2$, and 0.05% Brij35 pH 7.5 and MMP-8 was dialyzed against phosphate buffer saline (PBS). Each sample was diluted to 1 mg/mL and a volume of 1 mL. The dialyzed samples were analyzed in triplicate using a first-generation Apollo MMS system. For comparison purposes, the same samples were also run on the second-generation Aurora system. The Aurora instrument requires just 50 µL of sample, whereas Apollo requires approximątely 700 µL. In both systems, a backing pressure of 5 psi was applied to transfer the samples into the flow cell, where they were modulated at 1 Hz between sample and reference buffer (utilizing the same buffer used during dialysis) for background subtraction. The differential absorbance was measured within the range of 1588-1711 cm^{-1}. Replicates were averaged and all samples were normalized to obtain the absolute absorbance spectra.

Data processing in this study followed the procedures outlined in our previous application notes. Briefly, the raw differential absorbance data was transformed into absolute absorbance which is normalized by concentration and pathlength. Subsequently, the second derivatives of the absolute absorbance spectra were computed to enhance spectral features. The resulting plot was inverted and baselined, creating a "similarity plot" that qualifies the area of overlap when compared to a control, providing a measure of similarity between samples. Finally, employing Gaussian curve fitting, we fitted 11 Gaussians and calculated the higher order structure (HOS) based on the identification of different secondary structural elements across the amide I band (Table 1).

Table 1. Gaussian curve fit settings and HOS structural element designations.

Wavenumber (cm^{-1})	Secondary Structure	Wavenumber (cm^{-1})	Secondary Structure
1618	Beta-	1656	Alpha
1624	Beta-	1666	Turn
1632	Beta	1672	Turn
1638	Beta	1680	Turn
1642	beta	1688	Turn
1650	Unordered		

Results and Discussion

The MMS results reveal significant structural differences among the three MMP subtypes, MMP-2, MMP-8, and MMP-9 (Figure 3). Although all three proteins exhibit a mixture of alpha-helix (peaks at 1653-1658 cm^{-1}) and beta-sheet (peaks at 1636-1640 cm^{-1}) structures, as shown in Figure 3A, their peak positions and intensities are notably distinct. Additionally, all three spectra display less intense peaks at 1683-1687 cm^{-1} and at 1618-1624 cm^{-1}, representing the beta-turn and intermolecular beta-sheet structures, respectively.

Application Note
NOV 2023

Results and Discussion, continued

Interestingly, while one might expect MMP-2 and MMP-9 to have more similar structures due to their functional similarity, the MMS results suggest otherwise. MMP-2 and MMP-9 exhibit the most significant shifts, around 5 wavenumbers, for both the alpha-helix and beta-sheet peaks, whereas MMP-8 falls between the other two. In the case of the intermolecular beta-sheet peaks, MMP-9 displays a significantly more intense peak at 1624 cm^{-1}, which is 6 wavenumbers higher than MMP-2 and MMP-8 at around 1618 cm^{-1}. The relative abundance of these secondary structural elements in each protein was calculated using Gaussian curve fitting with the delta software and is presented in the HOS bar chart in Figure 3B. In all three proteins, the most abundant secondary structure is beta-sheet, followed by beta-turn and alpha-helix. Consistent with the similarity spectra, MMP-8 contains the most beta-sheet structures among the three proteins. MMP-2 has the most unordered structures and MMP-9 exhibits the most intermolecular beta-sheet structures (denoted as "beta-"). Despite their similar biological functions, it is evident that MMP-2 and MMP-9 do not share as much structural similarity with each other as compared to MMP-8.

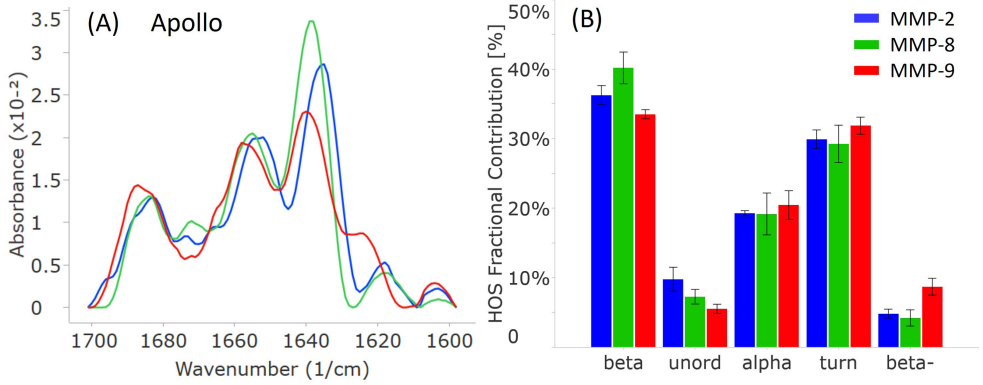

Figure 3. Apollo data showcasing the secondary structural comparison of MMP-2, MMP-8, and MMP-9. (A) Similarity plots (baselined second derivative spectra) illustrating the peaks within the amide-I band for each MMP. (B) HOS plot displaying the relative abundance of each secondary structural element for the MMPs. The error bars represent +/- the standard deviation (N=3).

For comparison, all 3 MMP samples were run on our second-generation instrument, Aurora. Figure 4A clearly shows that the distinct peak locations and intensities match the Apollo data. The HOS bar chart validates the HOS breakdown and the quality of data for Aurora (Figure 4B). In fact, the error bars and repeatability (Table 2) show that Aurora gives slightly higher data quality. This is due to our ability to have higher signal averaging with lower volume consumed per replicate.

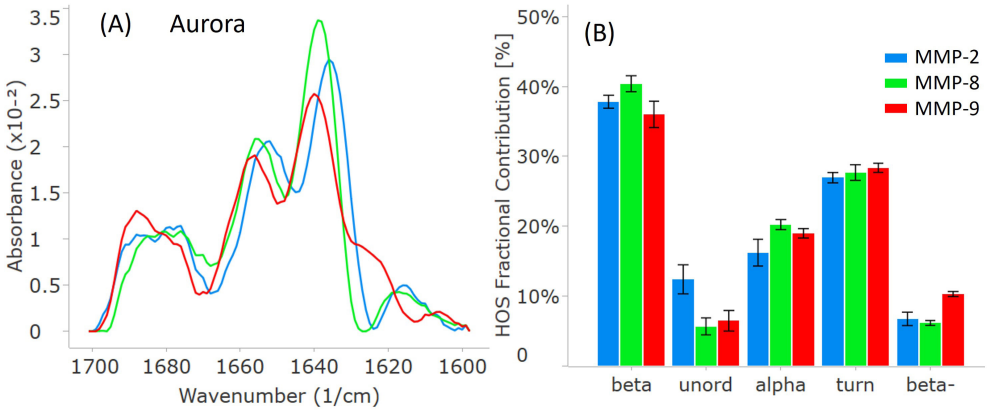

Figure 4. MMP secondary structure plots from the second-generation Aurora instrument. (A) Similarity plots (baselined second derivative spectra) illustrating the peaks within the amide-I band for each MMP. (B) HOS plot displaying the relative abundance of each secondary structural element for the MMPs. The error bars represent +/- the standard deviation (N=3).

Application Note
NOV 2023

Results and Discussion, continued

The quantification of structural similarity between the MMP proteins can be achieved by measuring the area of overlap (AO) between the similarity plots presented in Figure 3A and 4A. Table 2 provides information on the repeatability of the triplicate measurements within each sample and the sample-to-sample similarity in terms of percentage AO. To perform a comprehensive comparison, each MMP protein was taken as the control sample (indicated by 100% similarity) with the first similarity column using MMP-2, the second column using MMP-8, and the third column using MMP-9 as the reference. This highlights the concept of proteins being "similarly different" to one another. In other words, two proteins may share the same percent similarity to a third protein, yet they can still have different structures themselves, which is the case in this study. Table 2 reveals that no matter which protein is being compared to, the other two proteins always have relatively low (84-87% sample-to-sample similarity with 96-97% replicate repeatability, and >98% for Aurora) similarity scores, indicating again that all three proteins have distinct structures from one another.

Table 2. Repeatability of measurement and sample-to-sample similarity (the control for each similarity comparison is set at 100%). The top portion of the table is data from Apollo, and bottom is comparing data from Aurora.

Sample (Apollo)	Repeatability of triplicates	Similarity (MMP-2 control)	Similarity (MMP-8 control)	Similarity (MMP-9 control)
MMP-2	97.4%	**100%**	87.5%	86.0%
MMP-8	96.3%	87.5%	**100%**	85.3%
MMP-9	97.7%	86.0%	85.3%	**100%**
Aurora				
MMP-2	98.2%	**100%**	86.7%	84.7%
MMP-8	98.3%	86.7%	**100%**	86.0%
MMP-9	98.8%	84.7%	86.0%	**100%**

Most MMP isoforms, including those studied in this research, have a C-terminal hemopexin-like domain in their full-length protein following expression (proenzyme). As illustrated in Figure 5 (depicting MMP-9 as a dimer), this domain has four bladed beta-propeller structure composed of symmetrical blade-shaped beta-sheets. Typically, these beta-propeller structures are known to be involved in protein-protein interactions. MMP-9 therefore often exists in dimeric form. In our data, the presence of a small amount of intermolecular beta-sheet signals at 1618 and 1624 cm^{-1} suggests the possibility of dimerization or, more broadly, protein-protein interactions in all these samples in solution. This highlights the capability of MMS to investigate protein-protein interactions that involve the formation of intermolecular beta-sheets.

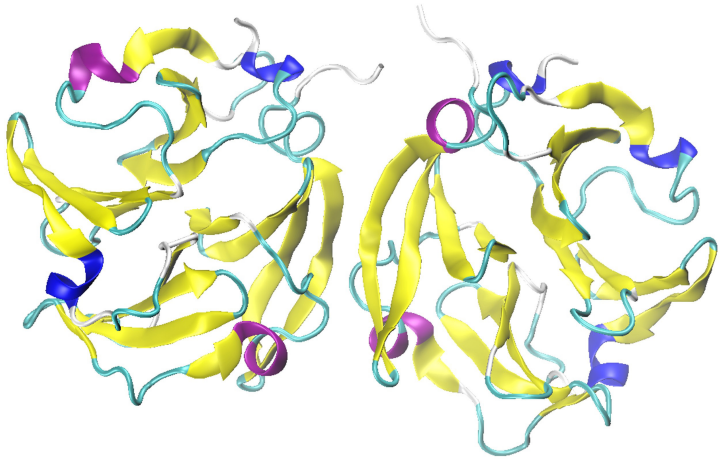

Figure 5. The hemopexin-like domain of MMP-9 in dimeric form (PDB: 1ITV).

Application Note
NOV 2023

Conclusions

In this study, we analyzed the proenzymes of three MMPs, MMP-2, -8, and -9, using two MMS systems: the Apollo and the Aurora. This is the first side-by-side comparison of data acquired from these two systems. Despite all three proteins belonging to the same MMP family, and both MMP-2 and MMP-9 being gelatinases, our MMS results revealed distinct secondary structures in these three proteins. Surprisingly, the structures of MMP-2 and MMP-9 were not more similar to each other compared to MMP-8, as activity would suggest. In fact, MMP-9 showed the most intermolecular beta-sheet structure and could provide insights to the hemopexin-like dimers. The observed structural variation in the proenzymes align with their respective crystal structures. These findings provide valuable insights into the structural relationship under formulation conditions between the proenzymes and active enzymes of MMPs.

Contributors

Richard Huang, PhD
Valerie Collins, PhD
David Gillingham

References

1. Verma, R. P., & Hansch, C. (2007). Matrix metalloproteinases (MMPs): Chemical–biological functions and (Q) SARs. *Bioorganic & medicinal chemistry,* 15(6), 2223-2268.

2. D Avila-Mesquita, C., *et al.* MMP-2 and MMP-9 levels in plasma are altered and associated with mortality in COVID-19 patients. *Biomed Pharmacotherapy*. 2021;142:112067.

3. da Silva-Neto, P. V., *et al.* Matrix Metalloproteinases on Severe COVID-19 Lung Disease Pathogenesis: Cooperative Actions of MMP-8/MMP-2 Axis on Immune Response through HLA-G Shedding and Oxidative Stress. *Biomolecules*. 2022;12(5):604.

4. Gelzo, M. *et al.* Matrix metalloproteinases (MMP) 3 and 9 as biomarkers of severity in COVID-19 patients. Sci Rep 12, 1212 (2022).

5. Kendrick, Brent S. *et al.* "Determining spectroscopic quantitation limits for misfolded structures." *Journal of pharmaceutical sciences* 109.1 (2020): 933-936.

6. Morgunova, E., Tuuttila, A., Bergmann, U., Isupov, M., Lindqvist, Y., Schneider, G., & Tryggvason, K. (1999). Structure of human pro-matrix metalloproteinase-2: activation mechanism revealed. *Science*, 284(5420), 1667-1670.

7. Bertini, I., Calderone, V., Fragai, M., Luchinat, C., Maletta, M., & Yeo, K. J. (2006). Snapshots of the reaction mechanism of matrix metalloproteinases. *Angewandte Chemie International Edition*, 45(47), 7952-7955.

8. Elkins, P. A., Ho, Y. S., Smith, W. W., Janson, C. A., D'Alessio, K. J., McQueney, M. S., ... & Romanic, A. M. (2002). Structure of the C-terminally truncated human ProMMP9, a gelatin-binding matrix metalloproteinase. *Acta Crystallographica* Section D: Biological Crystallography, 58(7), 1182-1192.